Hindawi
International Journal of Aerospace Engineering
Volume 2018, Article ID 2105682, 14 pages
https://doi.org/10.1155/2018/2105682

Research Article

Analysis of Global Sensitivity of Landing Variables on Landing Loads and Extreme Values of the Loads in Carrier-Based Aircrafts

Jin Zhou, Jianjiang Zeng, Jichang Chen, and Mingbo Tong

College of Aerospace Engineering, Nanjing University of Aeronautics & Astronautics, Nanjing, China

Correspondence should be addressed to Mingbo Tong; tongw@nuaa.edu.cn

Received 12 June 2017; Revised 26 October 2017; Accepted 9 November 2017; Published 14 January 2018

Academic Editor: Kenneth M. Sobel

When a carrier-based aircraft is in arrested landing on deck, the impact loads on landing gears and airframe are closely related to landing states. The distribution and extreme values of the landing loads obtained during life-cycle analysis provide an important basis for buffering parameter design and fatigue design. In this paper, the effect of the multivariate distribution was studied based on military standards and guides. By establishment of a virtual prototype, the extended Fourier amplitude sensitivity test (EFAST) method is applied on sensitivity analysis of landing variables. The results show that sinking speed and rolling angle are the main influencing factors on the landing gear's course load and vertical load; sinking speed, rolling angle, and yawing angle are the main influencing factors on the landing gear's lateral load; and sinking speed is the main influencing factor on the barycenter overload. The extreme values of loads show that the typical condition design in the structural strength analysis is safe. The maximum difference value of the vertical load of the main landing gear is 12.0%. This research may provide some reference for structure design of landing gears and compilation of load spectrum for carrier-based aircrafts.

1. Introduction

Carrier-based aircraft is the most important method for aircraft carrier strike group to control sea supremacy, and it is also an indispensable power for modern navies. Due to limited area in deck landing zone and the demand for bolting and go-around, carrier-based aircraft usually lands on deck via impact method under high sinking speed and high engaging speed along a fixed glide path angle [1]. The impact load, braking load of arresting cable [2, 3], and other loads at the moment when the aircraft touches deck put forward higher requirements for design and analysis of landing gears and airframe structure, especially for the structures closely related to landing [4].

At the primary design stage of an aircraft landing gear, the landing loads and the most severe landing conditions of the landing gear under different landing conditions should be determined according to design outline, which will be adopted in the parameter design of landing gear buffers and structural strength analysis. At the detailed design stage, optimization design will be carried out to balance performance and structure of the landing gear according to the relation between landing conditions and landing loads. Finally, the maneuvering envelope will be determined and the design of service load spectrum will be compiled for the assessment of fatigue life [5, 6].

At present, the research literatures and reports on definition of arrested deck landing conditions are mainly military standards and guides [7, 8]. MIL-A-8863C (AS) provides the landing variables, their distribution form, and empirical formula of mean value and standard deviation that should be considered in deck landing. Micklos [9] provided a measurement report on the landing variables of all kinds of carrier-based aircrafts landed on the Enterprise Aircraft Carrier in both day and night. The measurement of landing variables and loads is a costly and tedious task, thus a large amount of researches have been carried out on the simulation and analysis of landing dynamics to analyze different landing conditions and loads in recent years. Zhang [10] introduced deck motion into a dynamics model through the wheel-

deck coordinate system and simulated three landing situations to verify the model. Mikhaluk [11] and Lihua et al. [12] used finite element model to analyze forces on cables under different initial velocities and masses. Sati et al. [13] built a detailed aircraft arresting system using bond graph approach and studied the landing performance at different engagement speeds and masses.

The studies mentioned above give a simple trend of the relationship between landing variables and loads under a few landing conditions. However, the conditions empirically selected are unrepresentative. During the compilation of design service load spectrum, representative values of typical landing conditions can be obtained by discretizing the interval of landing parameters through sensitivity analysis. Incorrect structural load analysis may lead to excessive design, which would induce large weight and high cost at the primary stage of structure design. A further determination of the relationship between landing variables as well as the extreme value of the loads is required. Sebastian [14] analyzed the condition of free flight engagement (FFE), and the results show that the most severe loading condition of the landing gear takes place under the condition of free flight engagement at small sinking speed. Chester [15] researched the response of the main and nose gears via simulation of landing impact considering pitching and heaving degrees of freedom of the aircraft motion. The simulation indicates that the maximum vertical loads of main gears are almost linearly dependent on the sinking speed, while the response of nose gear is very sensitive to the initial values of pitch angle and pitching inertia. Yunwen et al. [16] explored the effect of different landing variables on sinking velocity based on the landing data measured from an E-2C. The results show that aircraft path angle and deck pitch angle are highly correlated with sinking velocity. Although they have studied part of the relevance between landing variables and loads, there is no direct conclusion on method accurate enough for determination of the representative values that can reflect typical landing conditions. Therefore, sensitivity and extreme value analysis need to be studied and it provides an important basis for the parameter design of landing gear buffer, structural optimization design [17], and fatigue analysis. However, theoretical basis and analysis method still need to be further investigated.

The extended Fourier amplitude sensitive test (EFAST) analysis method [18] is adopted in this paper to study the coupling and sensitivity between landing variables and landing loads. The method has been well applied in the field of hydrology [19], physical model [20], and so on. Based on military standards and guides, the effects of the multivariate distribution on the probability density function of single landing variable were analyzed and the distribution of single landing variable was fitted. By using the simplified landing virtual prototype and analysis of a large amount of landing conditions with the multicondition automatic simulation technology, the first-order and global sensitivity coefficients of landing variables on landing loads were calculated quantitatively, and the extreme value conditions and the frequency curves of the landing load were obtained.

2. Studies on Landing Variables in Military Standards

Many factors would affect the carrier-based aircrafts during the arrested deck landing. The landing variables and their relationships are mainly stipulated by related military standards and specifications.

2.1. Landing Variables and Multivariate Distribution. The military standard MIL-A-8863C (AS) stipulates the landing variables and their distributions. The condition of the landing variables needs to satisfy the demands of the multivariate distributions. The joint probability of the eight landing variables P_T is calculated by

$$\begin{aligned} P_T = {} & P\left(V_{TD}{}^{>}/_{<}V_{TDi}\right)P\left(V_E{}^{>}/_{<}V_{Ei}\right)P\left(V_V{}^{>}/_{<}V_{Vi}\right) \\ & \cdot P\left(\theta_P{}^{>}/_{<}\theta_{Pi}\right)P\left(\theta_R{}^{>}/_{<}\theta_{Ri}\right)P\left(\dot{\theta}_R{}^{>}/_{<}\dot{\theta}_{Ri}\right) \\ & \cdot P\left(\theta_Y{}^{>}/_{<}\theta_{Yi}\right)P\left(d^{>}/_{<}d_i\right), \end{aligned} \tag{1}$$

where V_{TD} is the approaching speed, V_E is the engaging speed, V_V is the sinking speed, θ_P is the aircraft pitching angle, θ_R is the aircraft rolling angle, $\dot{\theta}_R$ is the aircraft rolling rate, θ_Y is the aircraft yawing angle, and d is the off-center arresting distance. The subscript i denotes the initial value of each landing variable. The symbol ${}^{>}/_{<}$ is chosen to be either > or < according to the initial value of the variable. When the initial value of any landing variable is greater than the average one, the symbol > is chosen and it represents that the cumulative probability of that landing variable is greater than the initial value. Conversely, when the symbol < is chosen, it represents that the cumulative probability of that landing variable is less than the initial value.

The evaluation of the landing variables is determined by the extreme value of the cumulative probability P_0, namely,

$$P_0 = P(x > x_{\max\, i}) = P(x < x_{\min\, i}), \tag{2}$$

where $x_{\max\, i}$ and $x_{\min\, i}$ are the maximum and minimum value of the variables. In this paper, only the touch-and-go and arrested landing conditions are considered and the landing variables follow a normal distribution. The cumulative probability $P_0 = 1 \times 10^{-3}$, and the multivariate joint probability $P_T = 7.8125 \times 10^{-6}$.

2.2. The Effects of the Multivariate Distribution on the Landing Variables. The relationships among landing variables are according to the multivariate distribution. The product of the joint probability of the landing variables does not reflect the effects on the distribution of the single landing variable directly. Therefore, the distribution of landing variables is investigated according to the multivariate distribution.

Take the approaching speed V_{TD} as an example. There exists a relationship:

$$P\left(V_{TD}{}^{>}/_{<}V_{TDi}\right) \le P(\mu(V_{TD})) = 0.5, \tag{3}$$

where $\mu(V_{TD})$ is the average of the carrier engaging speeds. Take V_{TD} and V_E as an example. The extreme value of the

joint probability of any two landing variables is given by inserting (3) into (1).

$$P_T' = P\left(V_{TD}{}^{>}/_{<}V_{TDi}\right)P\left(V_E{}^{>}/_{<}V_{Ei}\right) \geq \frac{P_T}{0.5\cdot 0.5\cdot 0.5\cdot 0.5\cdot 0.5\cdot 0.5} = \frac{P_T}{0.015625} = 0.0005. \quad (4)$$

The distribution of the landing variable is mapped to a standard normal distribution in order to unify the range of the variables. The mutual effects among the value ranges of the landing variables are determined by the multivariate distribution [21]. In Figure 1, there are six equiprobable design envelopes of any two landing variables. The probability of each equiprobable envelope is shown in the figure.

The equiprobable envelope 6 represents the condition that the joint probability of two landing variables reaches the minimum, the value of which is $P_T' = 0.0005$. The equiprobable envelope 1 degenerates to a point which represents the condition that the joint probability of two landing variables reaches the maximum.

The evaluation of the eight landing variables of four groups on the equiprobable envelopes must ensure that the sum of their sequence number is nine, satisfying the demand of the joint probability. For example, when one group of variables is the equiprobable envelope 5, then other three groups must be the equiprobable envelope 1, 1 and 2.

It is difficult to make analytical calculations on the effects of the multivariate distribution on the single landing variable. Monte Carlo method is adopted to sample simulation for the complex probability constraints. Before sampling, the distribution of each variable should be mapped to the standard normal distribution. 10^5 simulate samples are extracted according to the distribution of each landing variable. The simulating sample screening is according to the multivariate distribution determined by (1). Figures 2 and 3 show the Monte Carlo sampling condition and the condition of applying multivariate distribution.

From the screening results, it can be seen that only 29,194 out of 10^5 samples remain after adopting multivariate distribution and the 71% of the samples cannot satisfy the requirements of the joint probability. By comparing Figure 2 with Figure 3, it can be known that the multivariate distribution deletes lots of samples that landing variables approaching the extreme value and keeps the samples that landing variables closing to the average. In Figure 3, the equiprobable envelope 6 is the envelope curve of the minimum value of the multivariate distribution shown in Figure 1.

The normal test is carried out by Kolmogorov-Smirnov method. $D = 0.005$, $P = 0.372 > 0.05$, and the landing variables after screening obey the normal distribution. The comparisons between distributions of landing variables before and after screening as well as the fitting conditions are shown in Figure 4. It is seen that after adopting the multivariate distribution, the probability density function of the single landing variable changes a lot.

From the analysis above, it is seen that the requirement of the multivariate distribution restricts the optional values

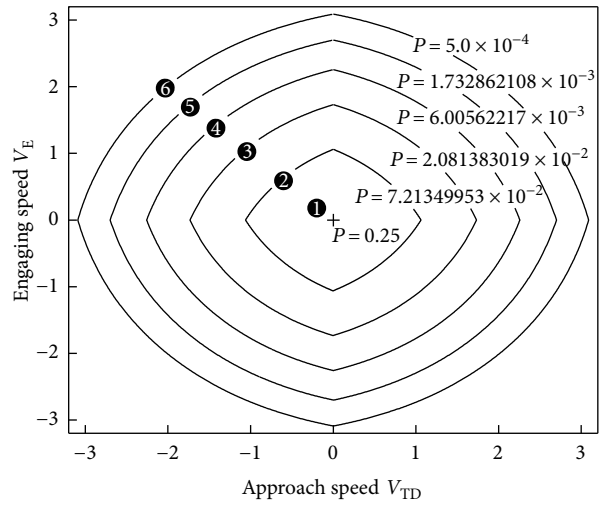

Figure 1: Equiprobable design envelope graph.

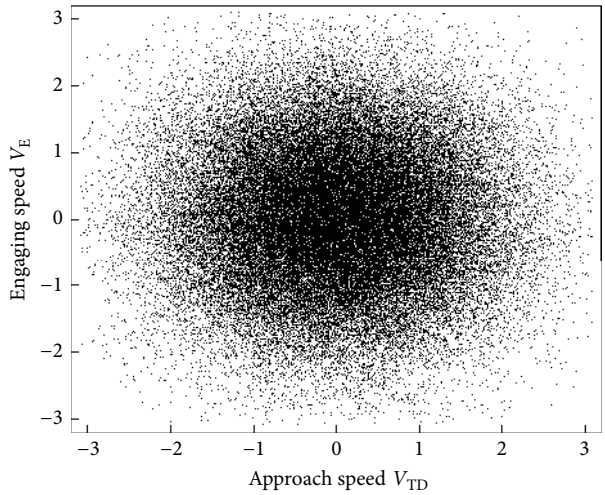

Figure 2: Multivariate Monte Carlo scatter diagram.

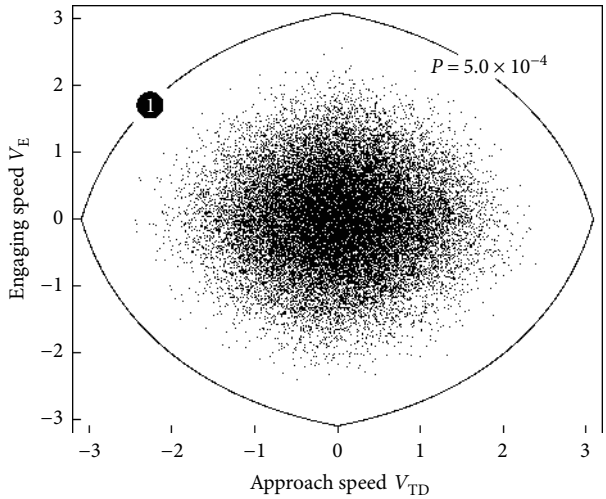

Figure 3: Multivariate distribution screening scatter diagram.

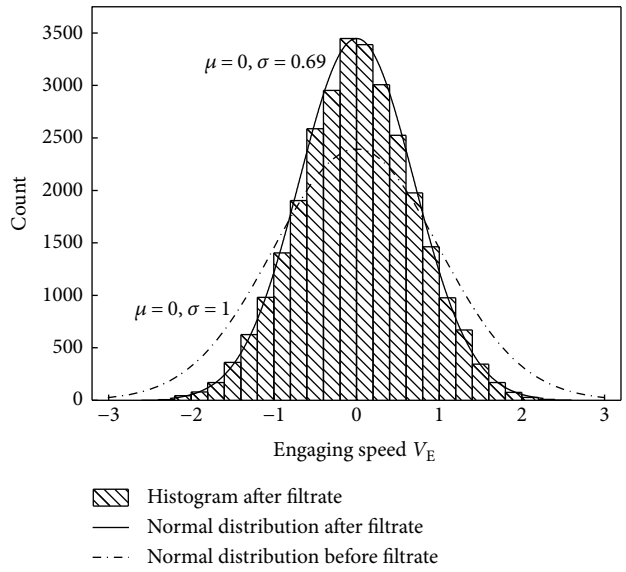

Figure 4: Comparisons of sample distributions before and after screening.

among the variables and has a large effect on the standard deviation of the single landing variable. The results of the sensitivity analysis are closely related to the probability density function of the input variables. The adoption of the distribution of the landing variables before their multivariate distribution would overestimate the probability that landing variables reach the maximum or minimum values, which may cause the errors of the global sensitivity analysis of the landing load. In this section, based on the requirements of the multivariate distribution, the equiprobable design envelopes of the landing variables are obtained. The distribution of the single landing variable for global sensitivity analysis is studied by Monte Carlo sampling method.

3. The Landing Virtual Prototype of the Carrier-Based Aircraft and the Multicondition Automatic Simulation

The attitudes of the aircrafts differ a lot at the moment of deck landing. Under the effects of the deck reacting force, the arresting force of the arresting hook, the aerodynamic force, and other forces, the load-time history of the landing gear is rather complicated during the landing process. The establishment of the accurate landing simulation model of the aircraft is the basis of the sensitivity analysis of the landing load. The accuracy of the sensitivity analysis is related with the sample quantity. In order to improve the reliability of the sensitivity analysis, it is necessary to consider the computation efficiency during simulating different landing conditions. The constraints and loads of the aircrafts during landing are analyzed, and the landing virtual prototype of the carrier-based aircraft based on LMS Virtual.Lab is established. For the computation efficiency problem of the massive landing conditions, the secondary development technology is applied to realize the multicondition automatic simulation and data processing of the landing conditions.

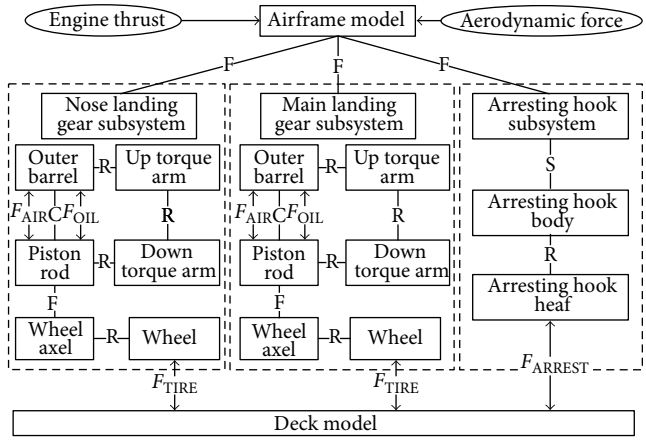

Figure 5: Landing virtual prototype constraints and loads. In the figure: R: swirl joint; C: cylindrical joint; S: spherical joint; F: fixed joint; F_{AIR}: air spring force; F_{OIL}: oil damping force; F_{TIRE}: tire force; F_{ARREST}: arresting force; omit the gravity.

3.1. Hypothesis of the Aircraft Virtual Prototype and Model Establishment. The aircraft virtual prototype consists of nose landing gear subsystem, main landing gear subsystem, arresting hook system, airframe model, and deck model. The external forces on the aircraft during landing are body load which includes aircraft gravity and engine thrust, aerodynamic force, acting force between tires, and deck and arresting force.

The virtual prototype has the following reasonable assumptions:

(1) Ignore the motion of the aircraft carrier and off-center landing.

(2) Assume that all components of the subsystems are rigid body, and the mass concentrates on the centroid.

(3) Ignore the effects of yawing landing on the arresting force curve.

According to the real motion of each component of the subsystems during the aircraft landing, the relating motion pairs such as swirl joint, cylinder joint, and spherical joint in subsystems are established. The constraints and load conditions of the subsystems are shown in Figure 5.

The initial condition of the virtual prototype is the moment that the aircraft lands on the deck, and the landing gears just touch the deck. During landing, the engine thrust maintains the maximum (twin engine). Arresting force-distance curve refers to military standards [8]. MK7-3 arresting machine is selected. The curve is obtained by weight interpolation and velocity compensation, shown in Figure 6.

The virtual prototype is established according to E-2 airborne early warning aircraft, shown in Figure 7.

3.2. Landing Multicondition Automatic Simulation. In order to improve the computation efficiency of the massive landing conditions, the automation technology is applied to realize the multicondition automatic simulation and data processing of the landing conditions. The auto-set, renewal, and analysis of the virtual prototype parameters are carried out by LMS

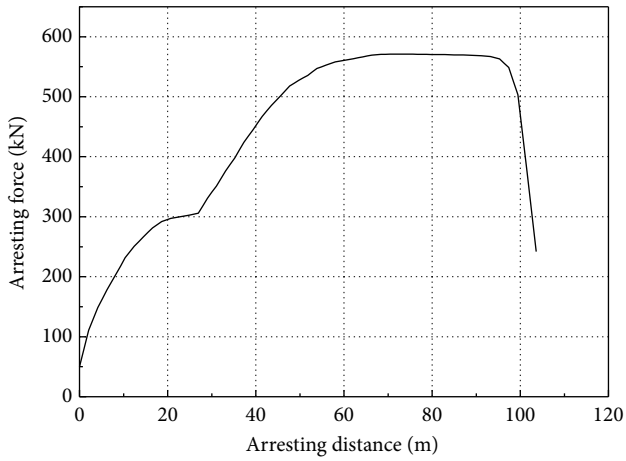

Figure 6: The arresting force-distance curve.

secondary development to realize the multicondition automatic simulation of the virtual prototype.

The virtual prototype of LMS Virtual.Lab motion can be divided into the product model and analysis model by function. The secondary development of the virtual prototype computes the initial landing attitude and location of the aircraft. The flow chart of the multicondition automatic simulation of the virtual prototype is shown in Figure 8.

Figure 7: Carrier-based aircraft landing virtual prototype.

The initial landing attitude of the carrier-based aircraft is determined by the multivariable pitching angle θ_P, rolling angle θ_R, and yawing angle θ_Y. The attitude transition matrix from airframe coordinate system to ground coordinate system is calculated by Tait-Bryan angles [22]. The transition matrix is used to update the aircraft attitude of the product model as follows:

$$L_{bg} = \begin{pmatrix} \cos\theta\cos\psi & \cos\theta\sin\psi & -\sin\theta \\ \sin\phi\sin\theta\cos\psi - \cos\phi\sin\psi & \sin\phi\sin\theta\sin\psi + \cos\phi\cos\psi & \sin\phi\cos\theta \\ \cos\phi\sin\theta\cos\psi + \sin\phi\sin\psi & \cos\phi\sin\theta\sin\psi - \sin\phi\cos\psi & \cos\phi\cos\theta \end{pmatrix}, \quad (5)$$

where the pitching angle $\theta = \theta_P$, rolling angle $\varphi = \theta_R$, and yawing angle $\psi = \theta_Y$.

When the aircraft attitude is determined, the aircraft location can be determined just with the constraints between the aircraft and the deck. When the rolling angle θ_R is positive, the aircraft tilts to the right and the right main landing gear just touches the deck, otherwise the opposite. The initial condition of the carrier-based aircraft includes the carrier engaging speed V_E, the sinking speed V_V, and the aircraft rolling rate $\dot{\theta}_R$. These variables can be set by analyzing the model. In the eight landing variables stipulated by military standards and guides, V_{TD} is not the variable at the moment of landing, so it cannot be considered in the virtual prototype. Besides, off-center condition is not taken into consideration. Therefore, both the ground critical velocity V_{TD} and off-center arresting distance d are simplified by using their average ones.

The sinking speed of the carrier-based aircraft is large during landing, and the landing gear bears rather large impact load. Referring to the analysis of the land-based landing load of the aircraft [23], the three directional loads of the landing gear and barycenter overload are selected as landing load to carry out the study. The course load and vertical load of the landing gear act on the center of the tire axle, while the lateral load acts on the contact point between the tires and the ground. The bounce landing is not permitted, so the maximum values of the three directional load and barycenter overload are selected as landing loads for analysis. After the BDF solver finishing solving the landing process, the extreme values of the three directional load and barycenter overload under this condition are output by calling the analysis model.

4. EFAST Global Sensitivity Analysis Method

During the aircraft landing, there are many landing variables and landing loads. The local sensitivity analysis method is limited by the variable selection and model, so the analytical results are usually not comprehensive or accurate enough. The variable range of the global sensitivity analysis can be extended to the entire variable domain, which can provide rather integrated quantitative analysis results. EFAST method is used to study the global sensitivity of the landing variables to the landing loads.

EFAST is the quantitative global sensitivity analysis method which is developed by Saltelli et al. [18]. Based on classical Fourier amplitude sensitivity test (FAST), Saltelli et al. combined Sobol variance decomposition thought to develop the method. This method maps the multidimensional variable to independent variable by appropriate searching curves. Then the search within the multidimensional variable

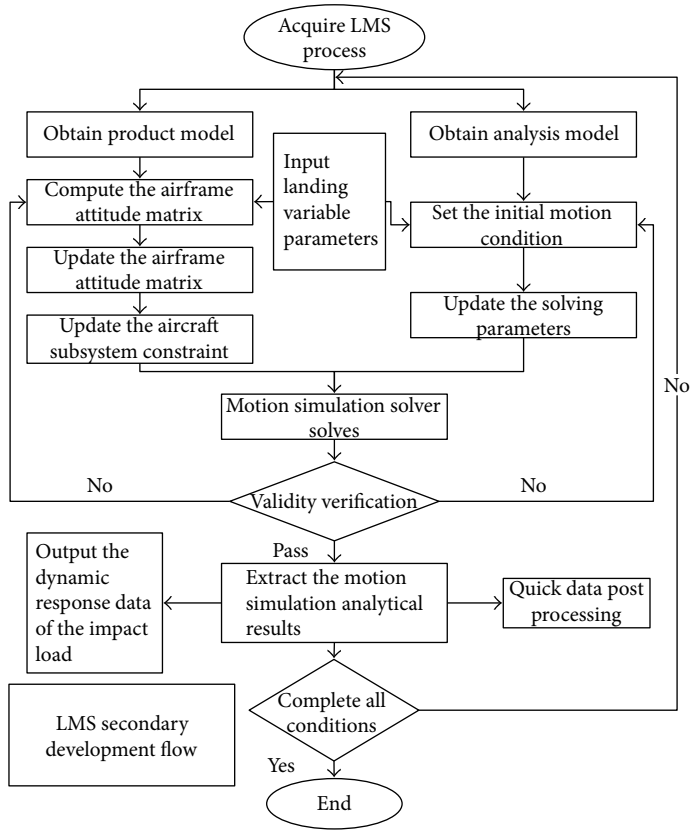

Figure 8: Flow chart of the virtual prototype multicondition automatic simulation.

space of the model is changed into the periodic function controlled by independent variable. Fourier transform is used to calculate the amplitude output by the model. The greater the change is, the more sensitive the variables are.

Assume that the landing analytical model is described as $y = f(X)$, where $X = X(x_1, x_2, \dots, x_n)$, $n = 6$ is the combination of the landing variables. Before performing the global sensitivity analysis, all variables have to be mapped to the interval [0, 1] to constitute the n-dimensional unit super cube space.

$$K^n = (X|0 \le x_i \le 1; i = 1, 2, \dots, n). \tag{6}$$

Define an independent variable s and introduce the same mapping $s \to X$, so

$$x_i(s) = G_i(\sin \omega_i s), \quad \forall i = 1, 2, \dots, n, \tag{7}$$

where $s(-\infty < s < +\infty)$ is the scalar variable, $\omega_i \in Z = \{-\infty, \dots, -1, 0, 1, \dots, +\infty\}$, and its value changes to suitable value according to x_i. With the change of s, all x_i change in the value space K^n. The oscillation frequency is ω_i. G_i is the searching curve and recommended by Sati et al. [13] as

$$x_i = \frac{1}{2} + \frac{1}{\pi}\arcsin(\sin \omega_i s + \varphi), \quad \forall i = 1, 2, \dots, n, \tag{8}$$

where φ is the random value in $[0, 2\pi]$.

Expand $f(X)$ by Fourier series.

$$\begin{aligned} y = f(X) &= f(x_1, x_2, \dots, x_n) \\ &= f(x_1(s), \dots, x_n(s)) \\ &= \sum_{j=-\infty}^{j=+\infty} \{A_j \cos js + B_j \sin js\}, \end{aligned} \tag{9}$$

where

$$\begin{aligned} A_j &= \frac{1}{\pi}\int_{-\pi}^{\pi} f(s)\cos jsds, \\ B_j &= \frac{1}{\pi}\int_{-\pi}^{\pi} f(s)\sin jsds. \end{aligned} \tag{10}$$

$j \in z = \{-\infty, \dots, -1, 0, 1, \dots, +\infty\}$, and the amplitude of the Fourier series is $\Lambda_j = A_j^2 + B_j^2$.

From the properties of A_j and B_j, it is known that $A_{-j} = A_j$, $B_{-j} = -B_j$, and $\Lambda_{-j} = \Lambda_j$. By calculating all frequencies, the total variance caused by each variable x_i can be obtained, namely,

$$V(E(y|x_i)) = \sum_{p \in Z^0} \Lambda_{p\omega_i} = 2\sum_{p=1}^{+\infty} \Lambda_{p\omega_i}, \tag{11}$$

where $Z^0 = Z - \{0\}$.

The total variance of the model is

$$V(E(y)) = \sum_{j \in Z^0} \Lambda_j = 2 \sum_{j=1}^{+\infty} \Lambda_j. \quad (12)$$

According to Sobol variance decomposition thought, the model can be decomposed into functions of single variable and combined variable, namely,

$$V(y) = \sum_{i=1}^{n} V_i + \sum_{i \neq j} V_{i,j} + \sum_{i \neq j \neq k} V_{i,j,k} + \cdots + V_{1,2,3,\ldots,n}, \quad (13)$$

where $V_i = V(E(y|x_i))$ which represents the variance of x_i, $V_{i,j} = V(E(y|x_i, x_j)) - V_i - V_j$ which represents the variance of x_i contributed by x_j, and $V_{i,j,k} \sim V_{1,2,\ldots,n}$ are by analogy. The first-order sensitivity coefficient S_{x_i} of the variable x_i is defined as below.

$$S_{x_i} = \frac{V_i}{V(y)}. \quad (14)$$

The total effects of the variable x_i include the single effect and interacting effects on the output of the model. The global sensitivity coefficient of the variable x_i is defined as

$$S_{x_i}^T = S_{x_i} + \sum_{i \neq j} S_{x_i,x_j} + \sum_{i \neq j \neq k} S_{x_i,x_j,x_k} + S_{x_1,x_2,\ldots,x_n}. \quad (15)$$

The difference between global sensitivity coefficient $S_{x_i}^T$ and first-order sensitivity coefficient S_{x_i} reflects the degree of interaction between x_i and other variables.

5. Landing Variable Sensitivity and Extreme Value Analysis

When using EFAST method to analyze the global sensitivity, the input of probability distribution of the variable and the output of the model corresponding to the inputting samples are required [18]. The landing variables given by standards [7] should be modified according to practical situation. The type of the landing variable distribution maintains constant, then the average and standard deviations of the landing variables need to be modified to satisfy the design requirements. Table 1 shows the distribution of the six landing variables under the given design requirements. Due to the effects of the deck layout, the value range of the rolling angle and yawing angle are not bilateral symmetric.

The input parameters of EFAST analysis method use the distribution of the landing variable and its value range obtained after adopting multivariate distribution presented in Section 2.2. The EFAST sampling is carried out by using (8), then 6438 samples are obtained. The samples in the generated interval [0, 1] are mapped back to the distribution of the landing variable, used to input the variables of the virtual prototype. For all landing conditions, the virtual prototype and its secondary development technology are used to analyze the landing loads automatically. According to the analytical results of the landing load, the first-order and global sensitivity coefficients of landing variables to landing loads are calculated.

Table 1: Aircraft landing variables distribution.

Landing variables	Mean	Deviation
V_E	166.164	9.26
V_V	3.5052	0.9184
θ_P	4.5	0.85
θ_R	2.2	2.5
$\dot{\theta}_R$	0	2.8
θ_Y	0.8	0.7

5.1. The Sensitivity Analysis of Main Landing Gear Load. When the carrier-based aircraft lands on the deck, main landing gear touches the deck first in most cases. The vertical impact load is the main load that acts on the main landing gear. The sensitivity analysis results of the vertical load of the main landing gear are shown in Figure 9.

The analysis results show that sinking speed and rolling angle are the main affecting variables of the vertical load of the main landing gear. The total contribution of the two variables is more than 82%, while the remaining landing variables only have little coupling effects on the vertical load. The sinking speed has larger first-order sensitivity coefficient in the analysis of the left main landing gear while the rolling angle has larger first-order sensitivity coefficient in the analysis of the right main landing gear. When the right main landing gear touches the deck first, the rolling angle is large and the landing load is relatively severe. When the left main landing gear touches the deck first, the rolling angle is small and the sinking speed is the main effect of the vertical load.

Figure 9 also shows the distribution of the cumulative frequency of the main landing gear's vertical load. The largest vertical load (853 kN) condition of the left main gear is $V_V = 4.76$ m/s and $\theta_R = -1.99^\circ$. The largest vertical load (1278 kN) condition of the right main gear is $V_V = 4.77$ m/s and $\theta_R = 7.09^\circ$. The extreme value of the vertical load of the right landing gear is 1.5 times of the one of the left landing gear.

The sensitivity analysis results of the main landing gear's lateral load are shown in Figure 10. It is seen that the sinking speed, rolling angle, and yawing angle are the main affecting factors of the main landing gear's lateral load. The total contribution of the three variables is over 91% while remaining variables barely have direct effects on the lateral load.

From the cumulative frequency curve of the lateral load shown in Figure 10, it is seen that the extreme value of the lateral load of the left main landing gear is nearly the same as that of the right main landing gear. However, the average load of the right main landing gear is larger than that of the left main landing gear. Under the condition that the largest lateral load of the left main landing gear is 120 kN, the sinking speed $V_V = 4.62$ m/s, rolling angle $\theta_R = 7.36^\circ$, and yawing angle $\theta_Y = 0.84^\circ$. Under the condition that the largest lateral load of the right main landing gear is 122 kN, the sinking

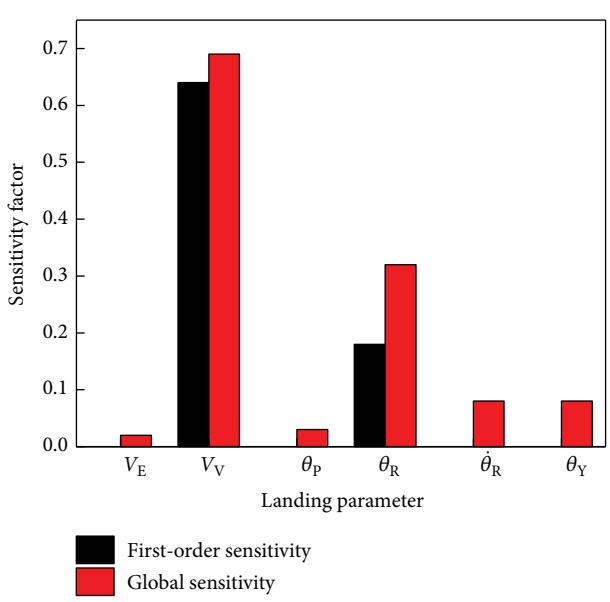

(a) Sensitivity factor of vertical load of the left main gear

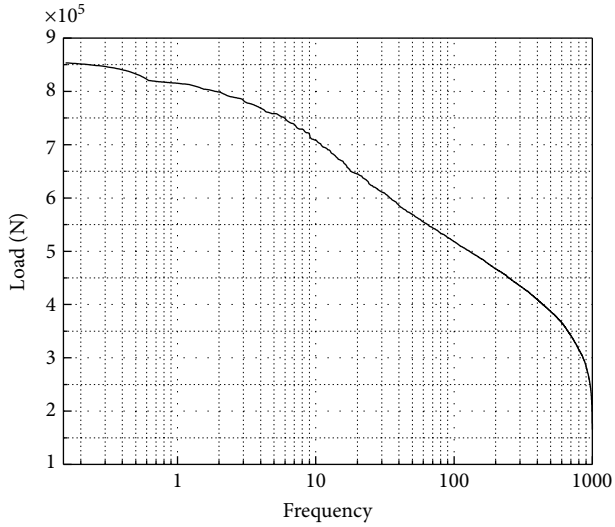

(b) Frequency curve of vertical load of the left main gear

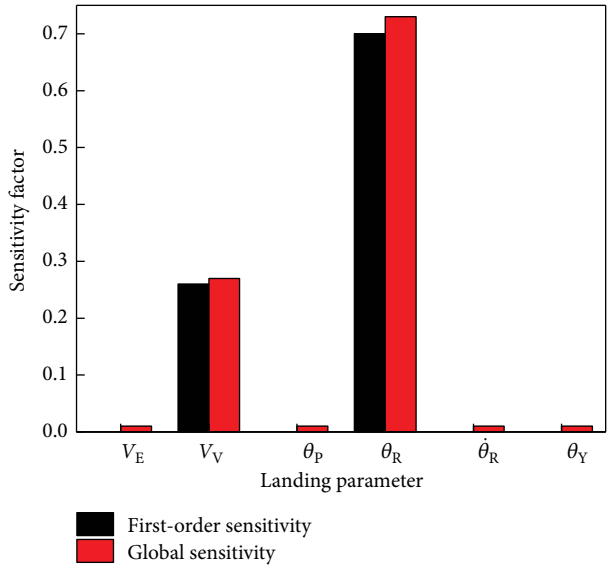

(c) Sensitivity factor of vertical load of the right main gear

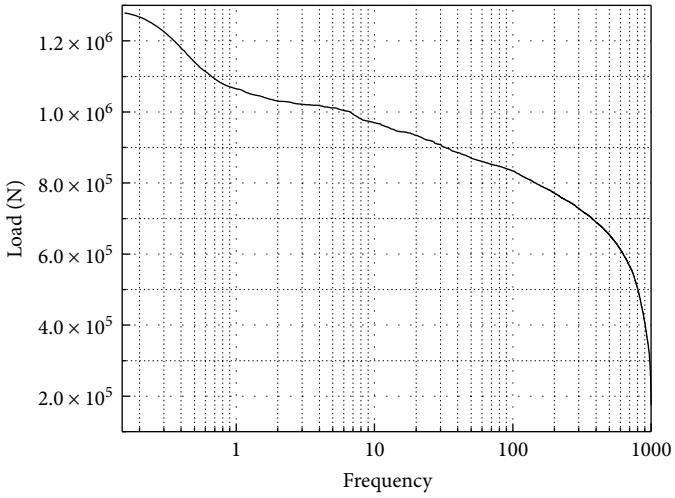

(d) Frequency curve of vertical load of the right main gear

Figure 9: Sensitivity and cumulative frequency curve of vertical load of the main landing gear.

speed $V_V = 4.61$ m/s, rolling angle $\theta_R = 7.36^\circ$, and yawing angle $\theta_Y = 0.84^\circ$.

The sensitivity analysis results of the main landing gear's course load are shown in Figure 11. The analysis results show that the sinking speed and rolling angle are the main affecting variables of the main landing gear's course load. The two variables' total contribution is 76% while the remaining landing variables have little coupling effects on the course load. Known from the cumulative frequency curve, the load distribution and extreme load of the left main landing gear is almost the same as that of the right main landing gear. Under the condition that the largest course load of the left main landing gear is 609 kN, the sinking speed $V_V = 4.59$ m/s and rolling angle $\theta_R = -2.04^\circ$. Under the condition that the largest course load of the right main landing gear is 721 kN, the sinking speed $V_V = 4.76$ m/s and rolling angle $\theta_R = 7.09^\circ$. The course loads of the left and right main landing gears have little difference. The extreme value of the course load also occurs under the condition of large sinking speed and large rolling angle.

Figures 9 and 11 show that the sensitivity analysis results of the course load are similar to that of the vertical load. The sensitivity coefficients of sinking speed and rolling angle are nearly the same. Besides, the course loads of the right main landing gear are all greater than that of the left main landing gear. The course load has rather high correlation with the vertical load.

5.2. Nose Landing Gear Load and Barycenter Overload Analysis. The sensitivity analysis results of the nose landing

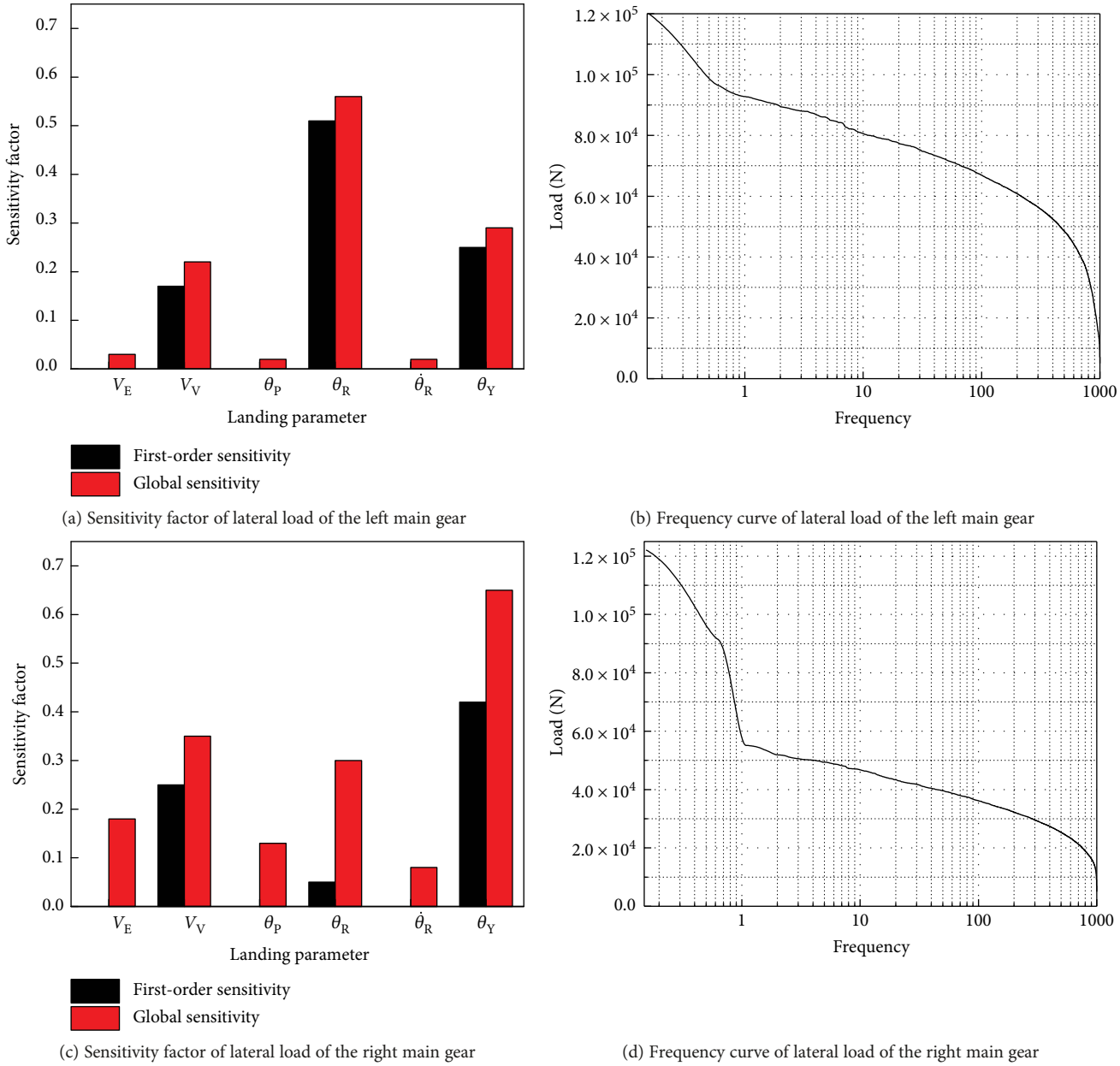

(a) Sensitivity factor of lateral load of the left main gear

(b) Frequency curve of lateral load of the left main gear

(c) Sensitivity factor of lateral load of the right main gear

(d) Frequency curve of lateral load of the right main gear

Figure 10: Sensitivity and cumulative frequency curve of lateral load of the main landing gear.

gear's three directional loads are shown in Figure 12. It can be known that the sinking speed and rolling angle are the main affecting variables of the nose landing gear's course load and their first-order sensitivity coefficients are 0.59 and 0.14, respectively. The pitching angle is the secondary affecting variable, and its first-order sensitivity coefficient is 0.004. Other variables have a few coupling effects on the course load.

For the lateral load of the nose landing gear, the rolling angle is the main affecting variable and its first-order sensitivity coefficient is 0.6. The sinking speed, pitching angle, and yawing angle have a few effects on the lateral load. For the vertical load of the nose landing gear, the pitching angle, rolling angle, and sinking speed are the main affecting variables and their first-order sensitivity coefficients are 0.53, 0.14, and 0.07, respectively. Other variables do not have appreciated effects on the vertical load.

From the cumulative frequency curve of the nose landing gear's three directional loads, the sinking speed $V_V = 5.41$ m/s, the pitching angle $\theta_P = 0.62^\circ$, and the rolling angle $\theta_R = 3.93^\circ$ under the condition that the largest course load of the nose landing gear is 133 kN. Under the condition that the largest lateral load of the nose landing gear is 93 kN, the sinking speed $V_V = 4.77$ m/s, the pitching angle $\theta_P = 3.09^\circ$, and the rolling angle $\theta_R = 7.09^\circ$, which is the large rolling angle condition. Under the condition that the largest vertical load of the nose landing gear is 196 kN, the sinking speed $V_V = 3.44$ m/s, the pitching angle $\theta_P = 6.23^\circ$, and the rolling

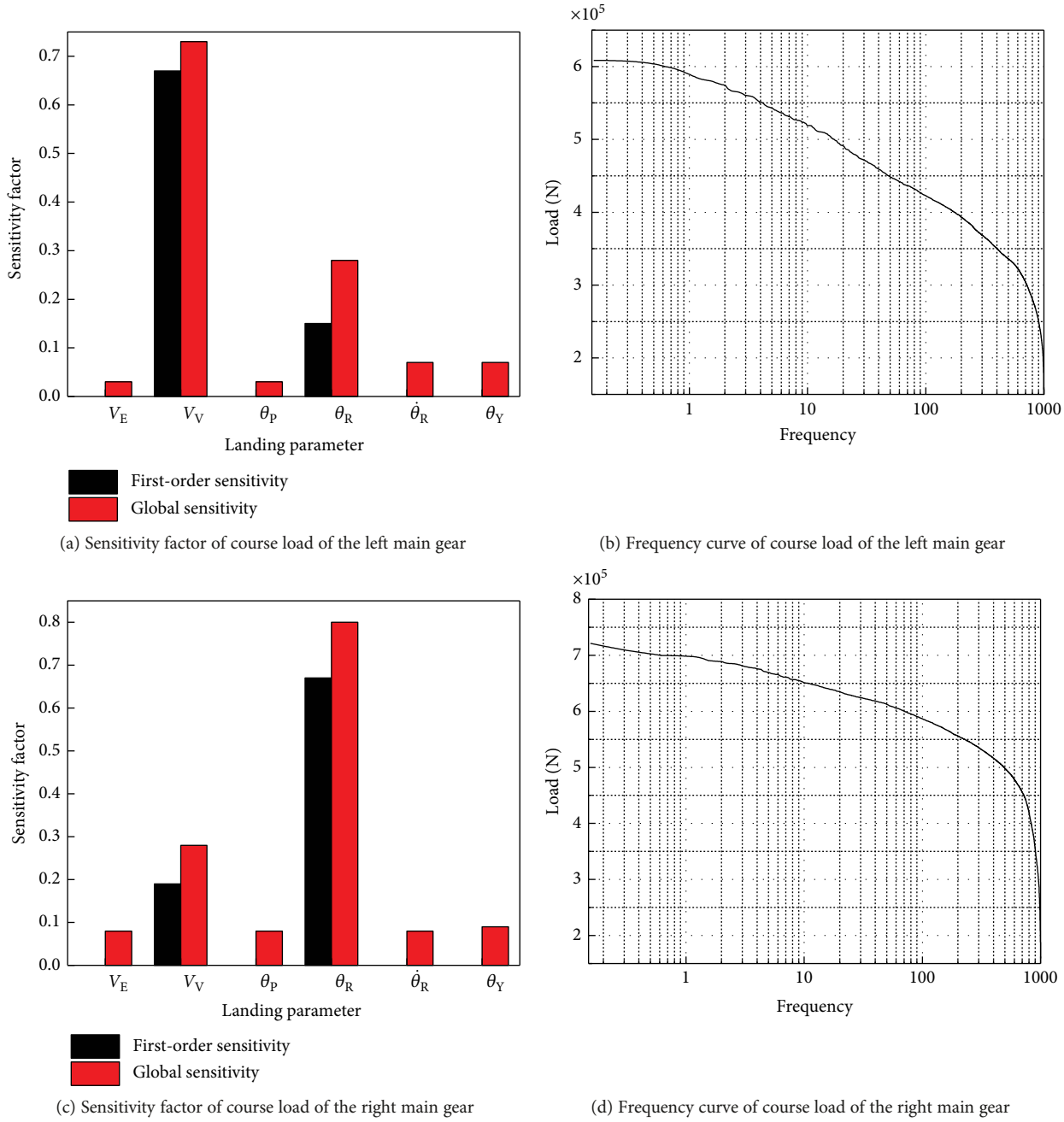

(a) Sensitivity factor of course load of the left main gear

(b) Frequency curve of course load of the left main gear

(c) Sensitivity factor of course load of the right main gear

(d) Frequency curve of course load of the right main gear

Figure 11: Sensitivity and cumulative frequency curve of course load of the main landing gear.

angle $\theta_R = 6.07^\circ$, which is the condition of medium sinking speed and large pitching angle.

The sensitivity analysis results of the barycenter overload of the airframe are shown in Figure 13. It is seen that sinking speed and rolling angle are the main affecting variables and their first-order sensitivity coefficients are 0.74 and 0.18, respectively. Under the condition that the largest barycenter overload is 5.11, the sinking speed $V_V = 4.77$ m/s and the rolling angle $\theta_R = 7.09^\circ$, which is the condition of large rolling angle and relatively large sinking speed. The barycenter overload of the airframe mainly concentrates between 2.0 and 4.0.

5.3. Sensitivity Analysis of the Landing Load of the Carrier-Based Aircraft. According to the sensitivity analysis results of the main landing gear, nose landing gear, and barycenter overload, the influence degree of the landing variables on landing loads can be classified as shown in Table 2. The sinking speed and pitching angle are the main affecting factors of the landing loads. The pitching angle and yawing angle have significant effects on some loads. The ground critical velocity and rolling rate have little effect on the landing loads, and they are influenced a lot by the change of the arresting cable load and the motion of the deck due to the restrictions of the simplified condition of the virtual prototype.

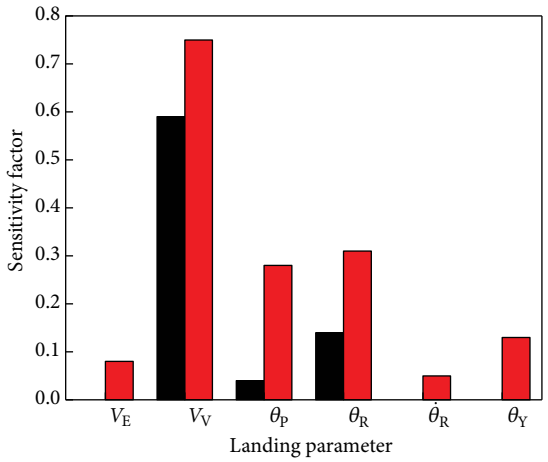

(a) Sensitivity factor of the course load of nose gear

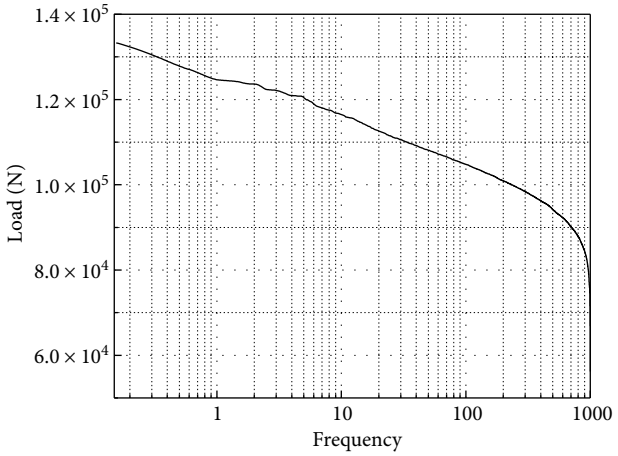

(b) Frequency curve of the course load of nose gear

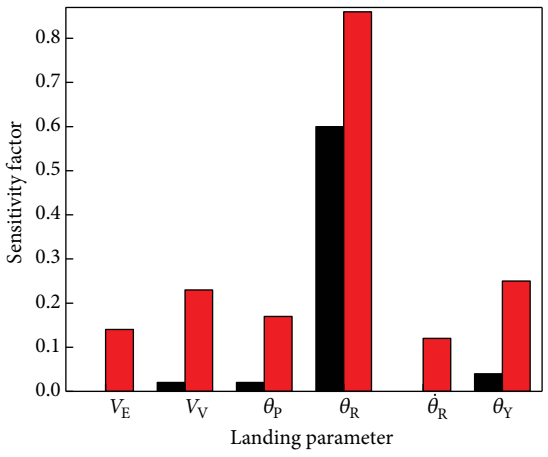

(c) Sensitivity factor of the lateral load of nose gear

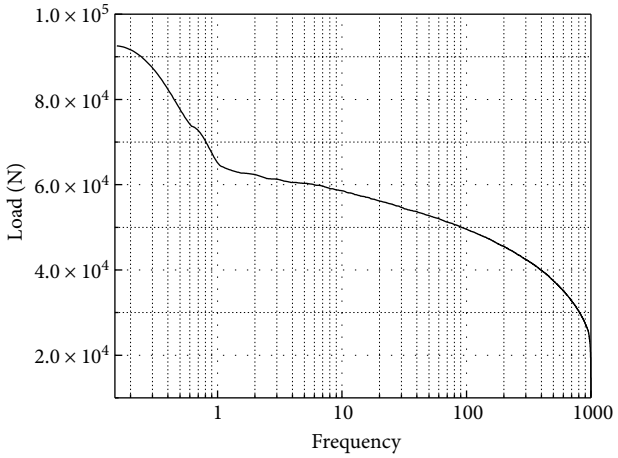

(d) Frequency curve of the lateral load of nose gear

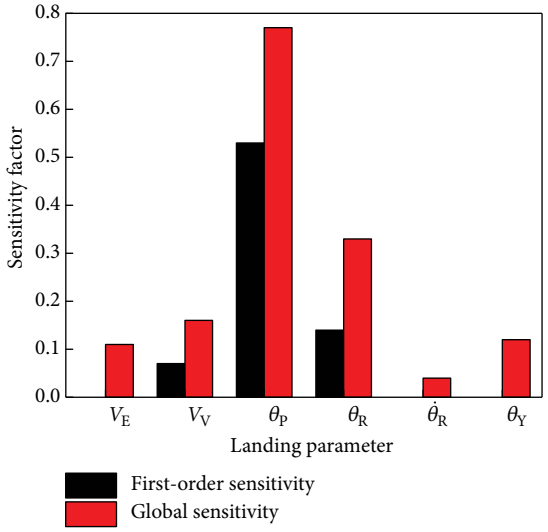

(e) Sensitivity factor of the vertical load of nose gear

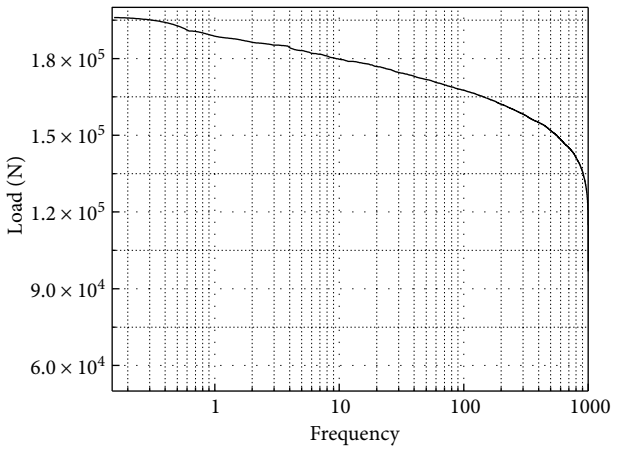

(f) Frequency curve of the vertical load of nose gear

Figure 12: Sensitivity and cumulative frequency curve of three directional loads of the nose landing gear.

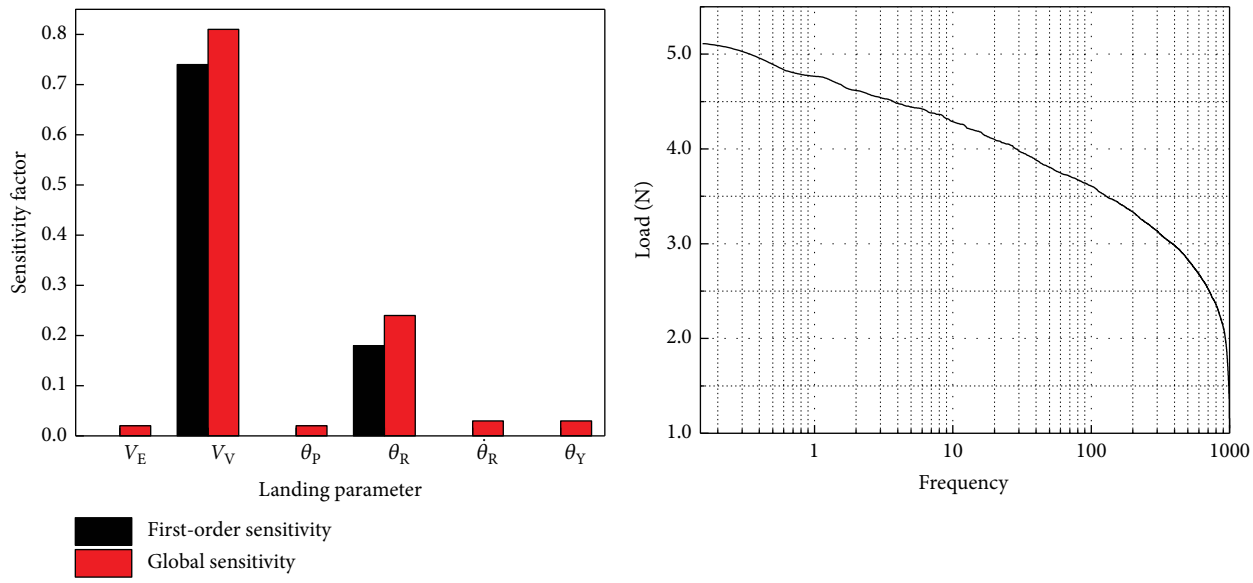

(a) Sensitivity factor of barycenter overload

(b) Frequency curve of barycenter overload

Figure 13: Sensitivity and cumulative frequency curve of the barycenter overload.

Table 2: Sensibility of landing variables to landing loads.

Type	High	Moderate	Low
Main gear	$V_V\theta_R$	θ_Y	$V_E\theta_P\dot{\theta}_R$
Nose gear	$V_V\theta_R\theta_P$	θ_Y	$V_E\dot{\theta}_R$
Gravity overload	$V_V\theta_R$	—	$V_E\theta_P\dot{\theta}_R\theta_Y$

When selecting the representative landing conditions of the carrier-based aircraft, the sinking speed, rolling angle, and pitching angle which have remarkable sensitivity should be discretized into several intervals. The intervals are selected to represent the values of variables. Different representative landing conditions are formed by the combination of the variables to reflect the landing load condition during the entire landing process.

5.4. Extreme Value Analysis of the Landing Loads of the Carrier-Based Aircraft. In the structure design stage, it is difficult to obtain the most severe load condition of the airframe during its service. When determining the most severe parameter combination, some conservative conditions are usually selected. For example, a certain or several extreme values of landing variables and the average of remaining landing variables are selected as extreme value conditions of the load for the researches. The conditions represent different landing conditions such as tail sinking, yawing landing, and landing with single landing gear. Some conditions will not happen during the service period, which leads to structural overdesign.

There are many landing samples selected in the sensitivity analysis of the landing load of the carrier-based aircraft. Approximately, the extreme load conditions of these samples can be used as extreme load conditions of all landing conditions to carry out the comparative analysis. From the computed results of the 6438 samples in EFAST sensitivity analysis method, the extreme value conditions of the three directional loads of the main and nose landing gear and barycenter overload are usually the condition that the sinking speed, rolling angle, or pitching angle are large and the landing variables do not pass the maximum of the value range. For further study in the rationality and security of the conservative condition design, typical condition design is selected for the comparative calculation.

Table 3 shows eight kinds of typical design conditions selected to compare with samples of EFAST sensitivity analysis in extreme loads of each direction. From the comparison, it is seen that the maximum gravity overload is slightly larger than that of the EFAST samples and the difference value is 23.5% approximately.

The extreme vertical and course loads of the landing gear of the typical design condition are nearly the same as the extreme values of EFAST samples. The maximum course load of the left and right main landing gear of the typical design condition is almost the same as the maximum load of the EFAST samples, and the percentage differences are about 6.2% and 16.0%, respectively. The maximum vertical load of the left and right main landing gear of the typical design condition is almost the same as the maximum load of the EFAST samples, and the percentage differences are about 2.5% and 12.0%, respectively. The maximum course and vertical loads of the nose landing gear of the typical design condition are quite different from the maximum loads of the EFAST samples, and the percentage differences are about 26.3% and 28.6%, respectively.

For the lateral load which is the secondary load, the maximum load of the typical design condition is quite different from that of the EFAST samples and the percentage difference is about 35.2%. From the overall analysis, the gravity overload and extreme load in each direction of the eight

Table 3: Extremum loads of typical landing conditions.

Condition of maximum variable (remaining variables are mean)	Gravity overload	Port main gear (kN)			STBD main gear (kN)			Nose gear (kN)		
		Course	Lateral	Vertical	Course	Lateral	Vertical	Course	Lateral	Vertical
V_V	5.5	564	81	787	692	40	1178	141	43	192
θ_R	3.9	340	63	398	586	52	1000	115	59	173
θ_P	2.8	328	53	371	459	26	645	113	33	195
$V_V\theta_R$	6.3	571	115	829	752	75	1431	166	74	219
$V_V\theta_P$	5.6	556	90	784	556	46	1166	140	46	215
$V_V\theta_R\theta_P$	6.2	564	118	827	649	75	1398	148	68	246
$V_V\theta_R\theta_Y$	6.2	564	158	832	836	69	1368	168	69	231
$V_V\theta_R\theta_P\theta_Y$	6.1	558	160	830	649	79	1333	154	84	252
EFAST samples	5.1	609	120	853	721	122	1278	133	93	196
Difference of maximum variable	23.5%	−6.2%	33.3%	−2.5%	16.0%	−35.2%	12.0%	26.3%	−9.7%	28.6%

kinds of typical design conditions are nearly the same as those of the EFAST samples, and the key loads of the typical design conditions are slightly larger. The extreme loads obtained by the conservative condition design are safe to be used in structure strength analysis and would not cause overdesign.

6. Conclusions

Based on the results reported, several conclusions can be drawn.

Firstly, the multivariate distribution has a large influence on the distribution of the landing variables. After multivariate distribution processing, the distribution of the landing variables is still close to the normal distribution, and the mean values of the variables maintain constant while the standard deviation decreases.

Secondly, the results of global sensitivity analysis show that all the six landing variables have effects on landing loads. The sinking speed and rolling angle almost influence all kinds of landing loads significantly and are the main affecting factors. The pitching angle and yawing angle may only influence some landing variables a lot, and they are the secondary affecting factors. The results of extreme value analysis show that it is safe to adopt typical condition design in the structural strength analysis.

Conflicts of Interest

The authors declare that there is no conflict of interest regarding the publication of this paper.

References

[1] S. A. Shappell and D. F. Neri, *The Effect of Combat on Aircrew Subjective Readiness and LSO Grades during Operation Desert Shield/Storm*, Naval Aerospace Medical Research Lab, Pensacola, FL, USA, 1992.

[2] B. N. Acharya, G. P. Gupta, S. Prakash, and M. P. Kaushik, "UV-resistant, water repellent and rodent repellent nylon tapes for aircraft arrester system," *Pigment & Resin Technology*, vol. 34, no. 5, pp. 270–274, 2005.

[3] D. T. Rusk, J. Pierce, W. Hoppe, B. Lancaster, R. Actis, and B. Szabo, *Analysis and Testing of Fleet Corroded F/A-18C/D Arrestment Shanks*, Naval Air Warfare Center Aircraft, Patuxent River, MD, USA, 2008.

[4] B. D. Flansburg, "Structural loads analysis of a carrier onboard delivery aircraft," in *57th AIAA/ASCE/AHS/ASC Structures, Structural Dynamics, and Materials Conference*, San Diego, CA, USA, 2016.

[5] N. S. Currey, *Aircraft Landing Gear Design: Principles and Practices*, American Institute of Aeronautics and Astronautics, Washington DC, USA, 1988.

[6] *Landing gear design loads*, Advisory Group for Aerospace Research and Development Neuilly-Sur-Seine, France, 1991, AD-A239 914.

[7] Naval Air Systems Command, *MIL-A-8863C (AS) Air-Plane Strength and Rigidity, Ground Loads for Navy Acquired Airplanes*, Patuxent River, MD, USA, Naval Air Systems Command, 1993.

[8] Naval Air Systems Command, *JSSG-2006 Aircraft Structures*, Patuxent River, MD, USA, Naval air systems command, 1998.

[9] R. P. Micklos, *Carrier Landing Parameters from Survey 45, Fleet and Training Command Aircraft Landing Aboard USS ENTERPRISE CVN-65 (Appendices B Through R)*, Naval Air Development Center, Warminster PA Air Vehicle and Crew Systems Technology Department, Warminster, PA, USA, 1991.

[10] Z. Wen, Z. Zhi, Z. Qidan, and X. Shiyue, "Dynamics model of carrier-based aircraft landing gears landed on dynamic deck," *Chinese Journal of Aeronautics*, vol. 22, no. 4, pp. 371–379, 2009.

[11] D. Mikhaluk, I. Voinov, and A. Borovkov, *Finite Element Modeling of the Arresting Gear and Simulation of the Aircraft Deck Landing Dynamics*, 2011.

[12] L. Lihua, W. Chen, and X. Panpan, "Dynamic analysis of aircraft arresting gear based on finite element method," in *2011 International Conference on System science, Engineering design and Manufacturing informatization*, pp. 118–121, Guiyang, China, 2011.

[13] S. C. Sati, A. S. Kanaskar, S. R. Kajale, and A. Mukherjee, "Modeling, simulation and analysis of aircraft arresting system using bond graph approach," *Simulation Modelling Practice and Theory*, vol. 19, no. 3, pp. 936–958, 2011.

[14] G. Sebastian, "Simulation of a free flight aircraft engagement during a carrier landing," in *35th Structures, Structural Dynamics, and Materials Conference*, Hilton Head, SC, USA, 1994AIAA-1994-1619- CP.

[15] D. H. Chester, "Aircraft landing impact parametric study with emphasis on nose gear landing conditions," *Journal of Aircraft*, vol. 39, no. 3, pp. 394–403, 2002.

[16] F. Yunwen, L. Sihong, X. Xiaofeng, C. Shuai, and P. Wenting, "Sinking velocity impact analysis of carrier-based aircraft based on test data," *Acta Aeronautica et Astronautica Sinica*, vol. 36, no. 11, pp. 3578–3585, 2015.

[17] M. Zhang, H. Nie, and Z. H. He, "Optimization parameters of nose landing gear considering both take-off and landing performance of catapult take-off carrier-based aircraft," *Transactions of Nanjing University of Aeronautics & Astronautics*, vol. 01, p. 12, 2016.

[18] A. Saltelli, S. Tarantola, and K. P.-S. Chan, "A quantitative model-independent method for global sensitivity analysis of model output," *Technometrics*, vol. 41, no. 1, pp. 39–56, 1999.

[19] M. Crosetto and S. Tarantola, "Uncertainty and sensitivity analysis: tools for GIS-based model implementation," *International Journal of Geographical Information Science*, vol. 15, no. 5, pp. 415–437, 2001.

[20] C. Xu and G. Z. Gertner, "A general first-order global sensitivity analysis method," *Reliability Engineering & System Safety*, vol. 93, no. 7, pp. 1060–1071, 2008.

[21] N. H. Sandlin, R. S. Ebers, and R. Black, "Ship motion effects on landing impact loads<149>V/STOL landing on aircraft carrier," in *20th Structures, Structural Dynamics, and Materials Conference*, St. Louis, MO, USA, 1979AIAA 79-0742.

[22] I. F. Mondragon, P. Campoy, C. Martinez, and M. A. Olivares-Mendez, "3D pose estimation based on planar object tracking for UAVs control," in *2010 IEEE International Conference on Robotics and Automation*, pp. 35–41, Anchorage, AK, USA, 2010.

[23] L. Kege and Y. Chuliang, "Load measurement and compilation of landing gear of airplane," *Acta Aeronautica et Astro-nautica Sinica*, vol. 32, pp. 841–848, 2011.